IL NUOVO CIMENTO **43 C** (2020) 140
DOI 10.1393/ncc/i2020-20140-2

COLLOQUIA: SIRR 2020

Coating thickness of plated objects using XRF technique concentrations

J. BROCCHIERI(*) and C. SABBARESE

Center for Isotopic Research on the Cultural and Environmental Heritage (CIRCE), Department of Mathematics and Physics, University of Campania L. Vanvitelli Caserta, Italy

received 25 January 2021

Summary. — The coating layer thickness of the double-layer objects was estimated using the concentration value of an element of the covering layer or of the substrate after obtaining suitable calibration curves using reference materials. The x-ray fluorescence technique was used with a handheld instrument to determine the concentration of elements. Various experimental configurations were built using gold- and silver-plated materials. The concentration calibrations curve as a function of coating layer thickness were successfully applied to gold-plated brass and copper jewelry, gold-plated samples and an ancient silver coin. The results obtained using the concentrations are in good agreement with those of other more elaborate methods.

1. – Introduction

The use of metal coatings on the surfaces of objects is a very common practice in different technological sectors [1,2] and in the field of cultural heritage [3,4] with the aim of protecting the surface, giving more value to the object or obtaining specific properties. Studies on them serve to highlight the true composition of the coating material, to provide information about the technology, production techniques and the mechanisms of union between the various layers of the artwork.

The direct measurement of coating thickness is rarely carried out under non-destructive conditions as it is generally a laborious procedure that is also prone to not small uncertainties. The use of theoretical or indirect thickness measurements is often preferred. For this reason, the use of a fast, non-destructive and accurate method to measure the thickness of the coating layer has been explored in several studies [5-9]. X-ray fluorescence was successfully applied by deriving the intensities of individual fluorescence peaks present in the spectrum and ratios between their intensities as a function

(*) Corresponding author. E-mail: jessica.brocchieri@unicampania.it

of the thickness of the coating material. X-ray fluorescence has been successfully applied by deriving the intensities of individual fluorescence peaks in the spectrum and ratios between their intensities as a function of the thickness of the coating material [10-13] and also considering the entire spectrum (see PLS method [14-16]).

The x-ray fluorescence technique allows the detection of chemical elements and their concentration in the surface layer of a sample. The constituents and their concentration of the surface layer depend on its analysed thickness. Characteristic fluorescence x-rays can be induced in both the coating and the substrate. The fluorescence x-rays of the underlying layer interacting with the overlay layer are attenuated. However, as the incident x-rays penetrate the sample, their intensity decreases, in particular those of lower energy are absorbed in the upper layer. By increasing the thickness of the coating, the low-energy portion is almost absorbed and only the high-energy portion reaches the deeper layers. The determination of coating thickness is a practice that has been carried out for decades by studying the intensity characteristic lines of the elements in the coating [17, 18] or measuring the intensity characteristic lines of the elements excited in the substrate [19-22] or, also, by simulation [8-10, 18] or multivariate analysis methods [14-16, 21].

The study was the estimation of the coating layer of double-layer objects using the concentration value of an element of the covering layer or of the substrate. Calibration curves were obtained from the concentrations measured with a handheld XRF spectrometer as a function of the coating layer thickness and using reference materials (built with different setups). The method of investigation, the setup configuration and the working conditions used to obtain the calibration curves were the same as those obtained in previous work [14-16]. The method was tested and compared to estimate the thickness of various to gold-plated brass and copper jewelry, gold-plated samples and an ancient silver coin.

2. – Materials and methods

Various setups were made by superimposing several thin sheets (a) of precious metal (gold or silver) on top of another thick metal (b), producing double layer samples (fig. 1).

This study makes use of the experimental works carried out in [14-16], but here only the concentrations of the elements present in the two layers is considered (quantity not used in previous works).

In particular, the several experimental setups are based on the following three configurations:

1) Fifty-nine square ($25 \times 25\,\mathrm{mm}^2$) 99.9% Au leaves were used. The thickness of a leaf measured was $(0.090 \pm 0.007)\,\mu$m. The gold leaves were superimposed to up to $5.2\,\mu$m. The materials covered by gold were silver, copper, iron and lead [15].

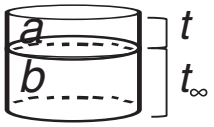

Fig. 1. – Layout of the measurement setup for a double layer: a is the precious metal layer of thickness t covering another metal b of thickness t_∞ (infinitely thick).

2) Forty-three 99.9% gold leaves were used. The thickness of a leaf was $(0.090 \pm 0.007)\,\mu$m. The leaves were carefully and gradually superimposed on a brass standard sample (Cu (57.87±0.06)%, Zn (38.29±0.05)%). The maximum gold thickness obtained was $3.87\,\mu$m [16].

3) Silver foils Ag (99.9 ± 0.3)% were used to cover metal plates (Cu, Fe, Pb). The thickness of the silver coating $(0.20 \pm 0.05)\,\mu$m was gradually increased up to a thickness of $14.5\,\mu$m [14].

Thicknesses of gold and silver leaves were measured by a thickness meter (Mahr Feinprüf Millitron nr. 1234 IC/Z) with a sensitivity of $0.01\,\mu$m. The overlapping of the foils (not always easy) was accurately done using non-metallic pliers.

Applications of methods were performed on gold-plated modern jewelry and on three gold-plated standard brass, copper and silver samples with an electrochemical process (galvanic gold plating). The objects were completely golden coated. Furthermore, the different methods were applied to estimate the surface enrichment thickness of an ancient silver coin.

XRF measurements were carried out using a XSORT XHH03 (Spectro) handheld spectrometer available at the CIRCE laboratory (`http://www.circe.unicampania.it`). The spectrometer is equipped with a Rh-target x-ray (configured to work with 50 kV and $125\,\mu$A) and a Si drift detector with $10\,\text{mm}^2$ active area and about 160 eV at the K_α line of the Mn (5.9 keV) energy resolution. The measurement time is 30 s (20 s using a 50 kV tube voltage and 10 s with 15 kV). Acquisition and analysis of XRF spectra were carried out using XRF Analyzer CE and XRF Analyzed PRO. MATLAB toolbox curve fitting environment was applied for fitting experimental data.

3. – Results and discussion

To estimate the thickness of plating in unknown samples using the handheld XRF instrument, several calibration methods were obtained. Calibration curves were derived using the concentrations obtained from XRF analysis on a series of reference samples with known thicknesses.

Figures 2 and 3 display the calibration curves obtained from the concentrations relative to the configuration 1) and 2) of sect. **2**. In each chart, the trends of the concentrations of the coated element and of the coating element as a function of the Au thickness are shown (fig. 2(a) Cu covered by gold, fig. 2(b) Ag covered by gold, fig. 2(c) Fe covered by Au and fig. 2(d) Pb covered by gold). Meanwhile, fig. 3 shows the trends in the concentrations of Cu and Zn present in the coated brass and Au in the coating layer.

The equations used to fit the concentration data of the substrate material (C) and the coating layer (C') *vs.* thickness (t) of the coating layer were respectively

$$C = a \cdot \left(e^{-b \cdot t}\right), \tag{1}$$

$$C' = c \cdot \left(1 - e^{-d \cdot t}\right). \tag{2}$$

The fit parameters of the five configurations of the double layer with gold are shown in table I. The first three columns show the values for the elements in the underlayer, while the remaining columns show the values for the gold overlay.

In fig. 2 the concentration trends of the elements in the substrate gold layers decrease rapidly when fluorescence energies are low, although this is not the case when gold covers silver (fig. 2(b)).

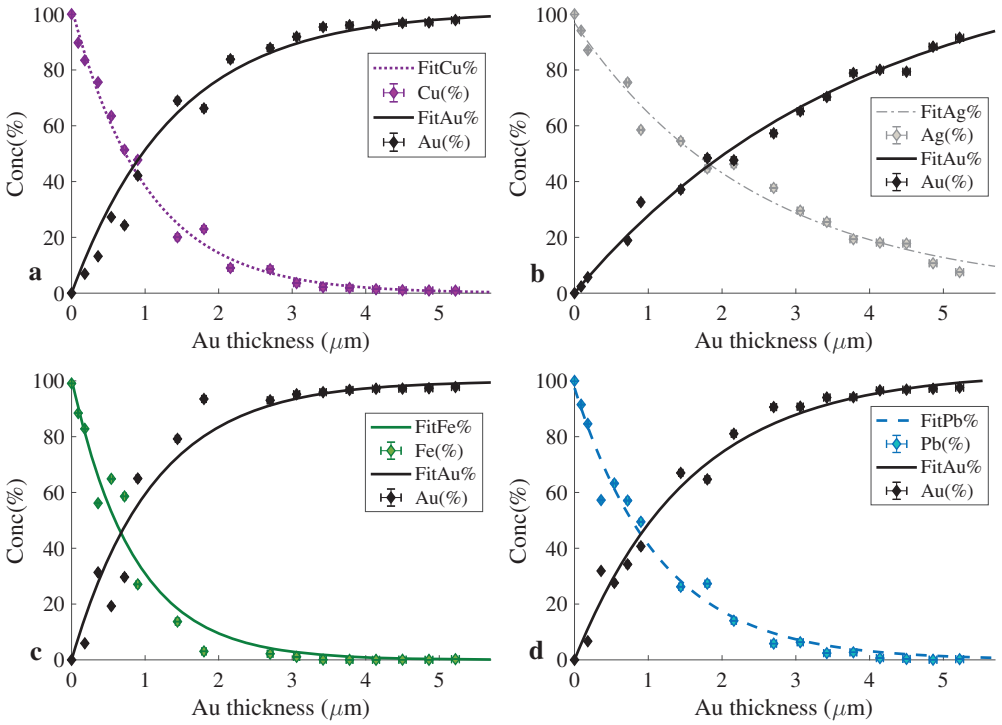

Fig. 2. – Trends in concentration values as a function of Au thickness in correspondence of four different substrates: (a) Cu; (b) Ag; (c) Fe; (d) Pb.

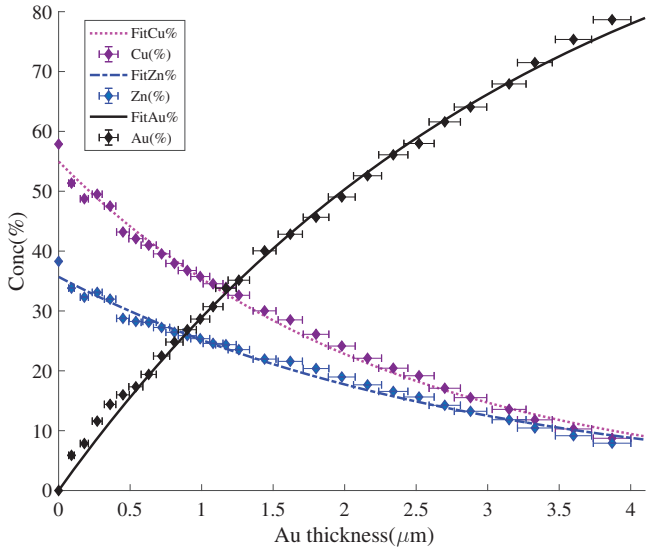

Fig. 3. – Concentration trends as a function of the Au thickness with brass substrate.

TABLE I. – *Fit parameters for eqs. (1) and (2) in the setups for the gold-coated sample configurations.*

	Fit parameters eq. (1)			Fit parameters eq. (2)	
	a (%)	b (μm^{-1})		c (%)	d (μm^{-1})
Cu	102 ± 6	0.98 ± 0.03	Au-Cu	101 ± 8	0.7 ± 0.2
Cu (brass)	55 ± 1	0.44 ± 0.01	Au-brass	111 ± 8	0.30 ± 0.03
Zn (brass)	35.7 ± 0.9	0.35 ± 0.02			
Ag	97 ± 5	0.41 ± 0.03	Au-Ag	122 ± 39	0.3 ± 0.1
Fe	100 ± 9	1.2 ± 0.2	Au-Fe	102 ± 9	0.8 ± 0.3
Pb	97 ± 6	0.9 ± 0.1	Au-Pb	104 ± 6	0.6 ± 0.1

Similar trends were obtained for two materials coated with silver, silver-plated copper and lead (fig. 4). Equations (1) and (2) were used for data fitting and the values of their parameters are shown in table II.

However, in the case of silver overlay, the attenuation does not occur very quickly because silver is less dense than gold. In fact, it can be seen in fig. 4(b) that with 15 μm of silver, the Pb concentration is not reduced to zero.

In all cases, the experimental data show few scattered dots due to the fact that sample surface has some roughness and non-uniformity, which increases the scattering of x-rays. The curves obtained were applied to gold and silver-plated objects and also to a silver enriched coin to estimate the thickness of the covering layer.

To validate the methodology here used, the thicknesses results were compared with those obtained using other methods previously applied [14-16], *e.g.*, the ratio of the characteristic lines of the elements present in the substrate, the cross ratios between the

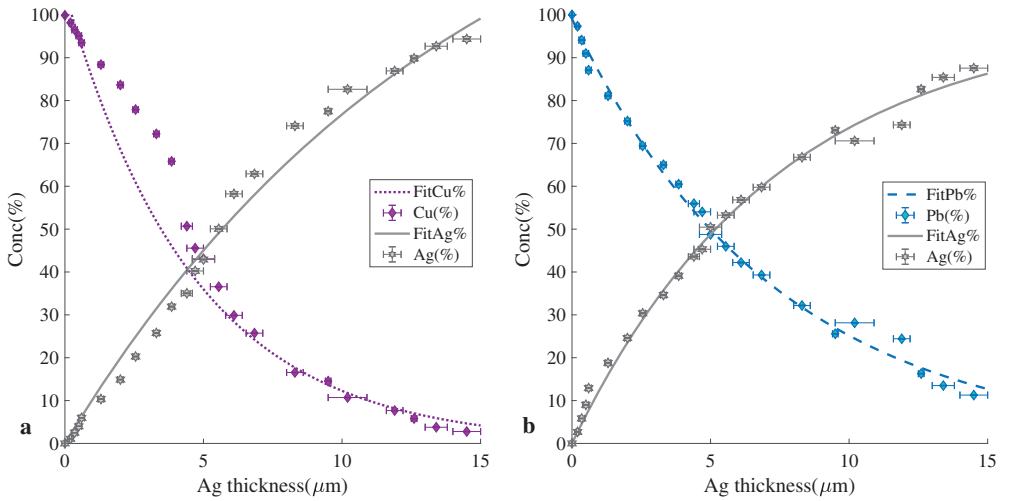

Fig. 4. – Concentration trends as a function of Ag thickness in two configurations: (a) Cu covered by Ag and (b) Pb covered by Ag.

TABLE II. – *The value fit parameters of the different configurations of the double layer with silver.*

	Fit parameters eq. (1)			Fit parameters eq. (2)	
	a (%)	b (μm^{-1})		c (%)	d (μm^{-1})
Cu	105 ± 5	0.215 ± 0.001	Ag-Cu	152 ± 29	0.07 ± 0.02
Pb	99 ± 2	0.135 ± 0.004	Ag-Pb	99 ± 5	0.13 ± 0.01

characteristic line of the element on the coating layer and the characteristic line of the element in the substrate and the PLS method.

Gold-plated jewelry Three gold-covered brass objects were analysed. They were Thunder Bracelet, Leaf Bracelet and Ring. The basic matrix of the jewelry was the same, but the gold covering was different. Indeed, the pieces of jewelry were composed of a brass alloy in which 60–77% was Cu and 3–7% was Zn coated with Au 7–25%. The thickness of these pieces of jewelry was estimated with both the calibration curves of the Au-coated copper and Au-coated brass configurations. This is due to the fact that the Zn concentration in the jewelry are lower than the standard used.

Oval Bracelet is a rigid oval shape bracelet gilded of copper. It was mainly composed of Cu (69 ± 5)%, Sn(16.8 ± 0.6)% and Au(5 ± 2)%. Therefore, the calibration curve used to estimate the thickness was the calibration curve for gold-coated copper.

The average of the thickness obtained with each different method is shown in table III: in detail, the estimated thicknesses via ratios of the Cu characteristic lines and the

TABLE III. – *The estimated thicknesses (in μm) of golden brass and copper jewelry via different methods. The last two columns report the result obtained here using the Au concentrations.*

Jewelry	$(t\_CuK_\alpha/K_\beta)^*$ [15]	$(t\_AuL_\alpha/CuK_\alpha)^*$ [15]	t_CuK_α/K_β [16]	t_AuL_α/CuK_α [16]
Thunder Bracelet	0.23 ± 0.06	0.33 ± 0.07	0.52 ± 0.04	0.19 ± 0.05
Leaf Bracelet	0.25 ± 0.06	0.28 ± 0.07	0.56 ± 0.04	0.14 ± 0.04
Ring	0.55 ± 0.08	0.67 ± 0.09	1.19 ± 0.04	0.6 ± 0.2
Oval Bracelet	0.23 ± 0.06	0.29 ± 0.08	–	–
	t_PLS [16]	t_Cu(%)	t_Au(%)$\_Brass$	
Thunder Bracelet	0.28 ± 0.05	0.38 ± 0.01	0.25 ± 0.03	
Leaf Bracelet	0.23 ± 0.05	0.29 ± 0.01	0.21 ± 0.03	
Ring	0.92 ± 0.05	0.56 ± 0.02	0.8 ± 0.1	
Oval Bracelet	0.21 ± 0.36	0.42 ± 0.01	–	

TABLE IV. – *The estimated thicknesses (in μm) of golden earring via four methods.*

Jewelry	t_AgK_α/K_β [15]	t_AuL_α/AgK_α [15]	t_PLS [15]	$t\_Au\_Ag(\%)$
Earring	0.33 ± 0.09	0.36 ± 0.02	0.34 ± 0.32	0.37 ± 0.15

TABLE V. – *The estimated thicknesses (in μm) of golden brass samples via five methods.*

Samples	t_CuK_α/K_β [16]	t_AuL_α/CuK_α [16]	t_AuL_α/ZnK_α [16]	t_PLS [16]	$t\_Au(\%)\_Cu$
Brass 1	0.03 ± 0.05	0.03 ± 0.01	0.02 ± 0.01	0.02 ± 0.05	0.03 ± 0.07
Brass 2	0.02 ± 0.05	0.04 ± 0.01	0.04 ± 0.01	0.04 ± 0.05	0.041 ± 0.004
Brass 3	0.05 ± 0.05	0.05 ± 0.01	0.05 ± 0.01	0.05 ± 0.05	0.048 ± 0.004

TABLE VI. – *The estimated thicknesses (in μm) of golden copper samples via four methods.*

Samples	t_CuK_α/K_β [15]	t_AuL_α/CuK_α [15]	t_PLS [15]	$t\_Au(\%)\_Cu$
Copper 1	0.17 ± 0.05	0.04 ± 0.02	0.08 ± 0.36	0.012 ± 0.004
Copper 2	0.16 ± 0.05	0.05 ± 0.02	0.09 ± 0.36	0.017 ± 0.005
Copper 3	0.10 ± 0.05	0.08 ± 0.02	0.09 ± 0.36	0.025 ± 0.008

cross ratio, the PLS method and concentration curve. The columns $(t\_CuK_\alpha/K_\beta)^*$ and $(t\_AuL_\alpha/CuK_\alpha)^*$ are the estimate of the thickness obtained from the calibration curve using copper standards [15]. The columns t_CuK_α/K_β, t_AuL_α/CuK_α and t_PLS report the estimates of the thickness obtained from the calibration curve using brass standards [16]. The last two columns show the thickness estimation using the calibration curve of the copper concentration in the Au-coated copper setup and using the calibration curve of the gold concentration in the Au-coated brass setup.

Earring was of gilded silver. XRF measurements detected that the object was composed mostly of Ag (78.9 ± 0.9)% and Au (11.2 ± 0.5)%. For this, the calibration curve for gold-plated silver was used. The average of the estimated thicknesses using the different methods is reported in table IV.

Gilded objects Three XRF measurements were also performed on the three standard golden samples with substrate of brass, copper and silver, respectively. Tables V, VI and VII show the averages of the thickness estimates obtained with the various methods studied in [14], [15] and [16] and that used here for the three setups, respectively: gold on brass, gold on copper and gold on silver.

Samples of different materials were plated simultaneously with three different plating

TABLE VII. – *The estimated thicknesses (in μm) of golden silver samples via four methods.*

Samples	t_AgK_α/K_β [14]	t_AuL_α/AgK_α [14]	t_PLS [14]	$t\_Au(\%)\_Ag$
Silver 1	0.08 ± 0.07	0.02 ± 0.02	0.04 ± 0.32	0.02 ± 0.01
Silver 2	0.05 ± 0.07	0.04 ± 0.02	0.06 ± 0.32	0.04 ± 0.02
Silver 3	0.05 ± 0.07	0.06 ± 0.02	0.05 ± 0.32	0.06 ± 0.03

TABLE VIII. – *The estimated thicknesses (in μm) of obverse and reverse sides of silver coins via different methods.*

Silver coin	t_CuK_α/K_β [14]	t_AgK_α/CuK_α [14]	t_PLS [14]	$t\_Ag(\%)\_Cu$
Coin_O	0.12 ± 0.45	0.5 ± 0.3	0.6 ± 0.3	0.3 ± 0.1
Coin_R	0.16 ± 0.45	0.5 ± 0.3	0.6 ± 0.3	0.3 ± 0.1

baths. The results showed that the different measuring times used for the electroplating process provided different thicknesses of gold. The longer the process the more gold is deposited on the standards. The estimates of gold thickness are approximately 0.03, 0.04 and 0.05 μm, respectively. Differences from various methods (tables V, VI and VII) are due to the fact that thickness values are comparable to or lower than the sensitivity of the methods. In fact, their uncertainties were almost equal to the estimated values because the gilding of these objects was extremely thin.

Silver coin Six XRF measurements were performed on the surface of the untreated coin on both the obverse and reverse sides [23, 24]. The coin is composed of Cu $(94.8 \pm 0.4)\%$ and Ag $(3.1 \pm 0.2)\%$ [14].

The average spectrum was used to estimate the thickness. The estimated thicknesses are shown in table VIII, where the calibration curves for the silver-coated copper setup were used.

The estimated thickness is therefore about $(0.4 \pm 0.3)\,\mu$m, in agreement with the thickness estimated on some coins belonging to the same mintage in [25].

4. – Conclusions

The thickness of an overlay material in a double layer experimental setup was determined using only the concentration of one element of the overlay or underlying layer. To obtain this result various calibration curves were obtained for different configurations with gold and silver materials. To derive the concentrations, XRF measurements were performed with a portable instrument. The results of the thicknesses were compared with those obtained with other methods using the fluorescence x lines of the same acquired spectra. The agreement between the data was good and showed that the method using concentration, although simple and more easily applicable, was equally valid.

REFERENCES

[1] Giurlani W. *et al.*, *Coatings*, **8** (2018) 260.
[2] Fiorini C. *et al.*, *X-Ray Spectrom.*, **31** (2002) 92.
[3] Trojek T. *et al.*, *Appl. Radiat. Isot.*, **68** (2010) 871.
[4] Cesareo R. *et al.*, *Nucl. Instrum. Methods Phys. Res., Sect. B*, **312** (2013) 15.
[5] Ulapane N. *et al.*, *NDT & E International*, **100** (2018) 108.
[6] Nygrd K. *et al.*, *X-Ray Spectrom.*, **33** (2004) 354.
[7] de Almeida E. *et al.*, *Spectrochim. Acta, Part B*, **167** (2020) 105818.
[8] Giurlani W. *et al.*, *Coatings*, **9** (2019) 79.
[9] Barcellos Lins S. *et al.*, *Appl. Sci.*, **10** (2020) 3582.
[10] Trojek T. *et al.*, *Radiat. Phys. Chem.*, **167** (2020) 108294.
[11] Cesareo R. *et al.*, *X-Ray Spectrom.*, **44** (2015) 233.
[12] Pessanha S. *et al.*, *Spectrochim. Acta, Part B*, **156** (2019) 1.
[13] Nardes R. C. *et al.*, *Radiat. Phys. Chem.*, **154** (2019) 74.
[14] Brocchieri J. *et al.*, *Nucl. Instrum. Methods Phys. Res., Sect. B*, **486** (2020) 73.
[15] Sabbarese C. *et al.*, *X-Ray Spectrom.* (2021) `https://doi.org/10.1002/xrs.3221`.
[16] Brocchieri J. *et al.*, to be published in *Nucl. Instrum. Methods Phys. Res., Sect. B* (2020).
[17] Brocchieri J. *et al.*, *Nuovo Cimento C*, **41** (2019) 224.
[18] Pessanha S. *et al.*, *Appl. Radiat. Isot.*, **152** (2019) 6.
[19] Barcellos Lins S. *et al.*, *Front. Chem.*, **8** (2020) 175.
[20] Karimi M. *et al.*, *X-Ray Spectrom.*, **38** (2009) 234.
[21] Lopes F. *et al.*, *X-Ray Spectrom.*, **45** (2016) 344.
[22] Cesareo R. *et al.*, *X-Ray Spectrom.*, **37** (2008) 309.
[23] Vitale R. *et al.*, *Ann. Ist. Ital. Numis.*, **64** (2018) 33.
[24] Brocchieri J. *et al.*, *Nucl. Instrum. Methods Phys. Res., Sect. B*, **479** (2020) 93.
[25] Doménech-Carbó M. T. *et al.*, *Sci. Rep.*, **8** (2018) 10676.